SCIENTIFIC REPORTS

OPEN

SUBJECT AREAS:
COORDINATION CHEMISTRY
KINETICS AND DYNAMICS

Received
8 May 2014

Accepted
9 October 2014

Published
29 October 2014

Correspondence and requests for materials should be addressed to J.-P.L. (jplang@suda.edu.cn)

In-situ X-ray diffraction snapshotting: Determination of the kinetics of a photodimerization within a single crystal

Fei-Long Hu[1], Shu-Long Wang[1], Jian-Ping Lang[1,2] & Brendan F. Abrahams[3]

[1]College of Chemistry, Chemical Engineering and Materials Science, Soochow University, Suzhou 215123, People's Republic of China, [2]State Key Laboratory of Organometallic Chemistry, Shanghai Institute of Organic Chemistry, Chinese Academy of Sciences, Shanghai 200032, People's Republic of China, [3]School of Chemistry, University of Melbourne, Victoria 3010, Australia.

In a single-crystal-to-single-crystal (SCSC) transformation, a preformed three-dimensional coordination polymer, $[Ni_3(oba)_2(bpe)_2(SO_4)(H_2O)_4]\cdot H_2O$ (H_2oba = 4,4′-oxydibenzoic acid; bpe = (E)-1,2-di(pyridin-4-yl)ethane) (1), was shown to undergo a [2+2] cycloaddition reaction upon exposure to UV irradiation. The kinetics of this reaction were followed by taking "snapshots" of the solid state transformation using *in situ* single crystal X-ray crystallography; a first order process was indicated. The reaction rate was influenced by many factors such as the separation of the sample from the UV light source, the heat produced by the UV irradiation, the light flux of the UV lamp used, the size of the single-crystal and the powder samples. The investigation of the kinetics was complemented by ^{1}H NMR studies. The results clearly demonstrate that *in situ* single-crystal X-ray diffraction is able to provide useful insights into the gradual formation of the photoproducts and the reaction processes. The work also offers a clear indication that it is possible to use the technique to study the kinetics of other photocycloaddition reactions and SCSC processes in general.

In recent times solid-state reactions involving inorganic and organometallic compounds have attracted considerable interest because of their importance in the area of green chemistry[1–2]. Moreover, solid-state reactions can be useful in generating products that are difficult to obtain using solution reaction methods[3–5]. Although there are advantages associated with the use of solid state reactions the employment of such a synthetic approach brings significant challenges. For example, the solid state reactions do not always occur in a controllable manner[6–8] or are incomplete at ambient temperature[9]. In many cases, the products are formed in relatively low yields (20–30%) and contaminated with unreacted starting materials, side-products, and even some intermediate species, making it extremely difficult to identify and isolate the desired products from the solid state mixture. Although recrystallization in solvents may assist in the isolation of the product from the solid state mixture, there is a possibility that the isolated product is not the species generated in the solid state[10]. Furthermore, the limited availability of appropriate analytical techniques makes it difficult to follow the progress of solid-state reactions. Routine analytical techniques such as IR, ^{1}HNMR, UV-vis etc. which are commonly used to monitor the real-time generation of products in solution reaction are not easily employed in the identification of products arising from solid state reactions[11]. Finally, determining the mechanism of a solid state reaction is problematic because of the difficulty in probing the reaction kinetics[12]. In summary, investigations of solid state reactions and the accompanying kinetics[13] using suitable real-time methods represent a considerable challenge.

Single-crystal-to-single-crystal (SCSC) transformations represent a special type of solid-state reaction which can be initiated by light or heat, or alternatively by the removal, uptake or exchange of guest molecules. SCSC transformations provide fascinating examples of solid state reactions and represent a current topic of considerable interest in solid-state chemistry[14–17].

Single-crystal X-ray diffraction is the primary tool currently employed to identify the final products of these transformations in the solid state[18]. In order for the structural transformation to occur, the single crystal has to withstand the stress accompanying internal rearrangements with retention of its single crystal character[19–23]. Thus the technique of single crystal X-ray diffraction is only going to be useful for probing these transformations when the structural changes during the reaction are relatively small[24–25].

In 2009 Fujita and co-workers, using single crystal X-ray diffraction to follow the reaction, reported a transient hemiaminal trapped in a porous network[23]. Very recently, Yang and co-workers employed a similar approach to monitor the progress of a [2+2] photodimerization involving the C=C bonds of a 1,4-bpeb guest molecule and the C=C bonds of 1,3-pda ligands which form part of a framework that has the overall composition of $\{[Mn(1,4\text{-bpeb})(1,3\text{-pda})]\cdot(1,4\text{-bpeb})\}_n$ (1,4-bpeb = 1,4-bis((*E*)-2-(pyridin-4-yl)vinyl)benzene; 1,3-pda = 1,3-phenylenediacrylic acid)[26]. Despite the clear insights provided by the structural analyses, details relating to the kinetics and mechanism of the [2+2] cycloaddition reaction were rarely reported[27–31].

Solid state [2+2] photodimerization of alkenes in various organic compounds and metal complexes have been the subject of much investigation over the past decade[32–38]. Recently, ditopic spacer ligands such as bpe and 1,4-bpeb have been found to undergo photo-cycloaddition in SCSC processes[39–48]. With respect to these transformations in coordination polymers, Vittal and co-workers have made significant contributions that provide clear insights into the processes as well as offering an indication of the scope and applicability of the [2+2] photo-cycloadditions[49–50]. Despite the excellent work done by MacGillivray[1,3], the isolation of photoproducts formed at different irradiation time intervals has been difficult to achieve and the kinetics of such processes remains unclear[51–54].

Under solvothermal conditions we have carried out a reaction of $NiSO_4\cdot 7H_2O$ with bpe and H_2oba and isolated a three-dimensional coordination polymer of composition $[Ni_3(oba)_2(bpe)_2(SO_4)(H_2O)_4]\cdot H_2O$ (**1**). As discussed later in this paper, all C=C bonds within the network are found in a single crystallographic environment and each is in relatively close proximity to a symmetry-related C=C bond. This arrangement in which the only atoms likely to participate in a [2+2] cycloaddition are clearly identified provides an opportunity for studying the kinetics of the photocycloaddition reaction. In this work, we investigate a SCSC [2+2] cycloaddition reaction by *in situ* single-crystal X-ray diffraction. By taking crystallographic "snapshots" of the transformation at various time intervals, the kinetics of the process can be examined. Supported by powder X-ray diffraction (PXRD) and ^{1}H NMR measurements, the results show that the [2+2] photocycloaddition reaction exhibits first-order reaction behavior in the solid state.

Results

Synthesis and structural characterization. Compound **1** was obtained by solvothermal reaction of $NiSO_4\cdot 7H_2O$ with bpe and H_2oba in a molar ratio of 1 : 1 : 1 at 145°C. The thermal stability of **1** was investigated by thermogravimetry (Supplementary Fig. S1). The TG curve of **1** displayed the first weight loss stage at *ca.* 182°C (obsd. 6.28%; calcd. 7.26%), which was assigned to the loss of the lattice and coordinated water molecules. The second weight loss of 60% in the temperature range of 400 to 520°C corresponded to the decomposition/loss of the ligands. The PXRD patterns of the bulk products of **1** are well-matched with the simulated ones generated from the single-crystal X-ray diffraction data (Supplementary Fig. S2).

Compound **1** crystallizes in the *C*2/*c* space group and its asymmetric unit contains half a $[Ni_3(oba)_2(bpe)_2(SO_4)(H_2O)_4]$ unit and one water lattice molecule. A trinuclear cluster is formed as indicated in Fig. 1a. There are two octahedral Ni2 centres in each cluster and each is coordinated by *cis*-carboxylate oxygen atoms (O5 and O9), a nitrogen atom (N1) from a bpe ligand, an oxygen atom (O2) from a bridging sulfate anion and the oxygen atoms (O3 and O4) of two *cis* water molecules. Ni1 is also in an octahedral environment formed from two *trans* nitrogen atoms (N2) belonging to two bpe ligands, oxygen atoms (O2) of a chelating sulfate anion and two *cis* oxygen atoms belonging to two separate carboxylate groups. A 2-fold axis passes through S1 and Ni1. Four bis(carboxylate) oba^{2-} ligands serve as bridges to four equivalent trinuclear Ni clusters to generate a 2D 4,4-network with nodes approximately 19Å apart. Pairs of bpe ligands extend above and below the trinuclear clusters to form a 3D network. The distance between the nodes separated by the bridging bpe ligands is approximately 14 Å. If each pair of bpe ligands, that extends both above and below the trinuclear cluster, is treated as a single bridge, then each trinuclear cluster may be considered as a 6-connecting node within a 3D network possessing the

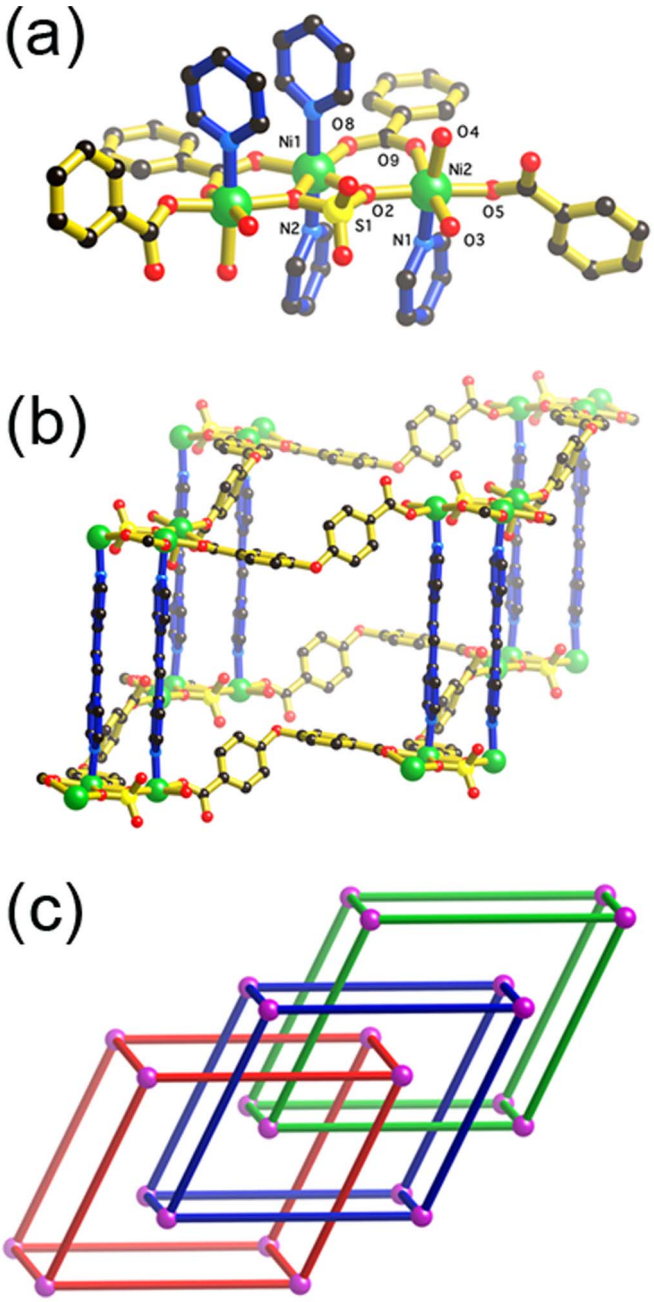

Figure 1 | Representations of compound 1. (a) View of the trinuclear cluster; C black, N blue, O red, Ni green; bpe bonds are indicated with blue connections; H atoms have been omitted for clarity. (b) Part of a single network showing a trinuclear unit bridged by either oba ligands or pairs of bpe ligands; colour scheme as for part (a); H atoms have been omitted for clarity. (c) Schematic representation of the interpenetrating networks; nodes are represented by pink spheres; the rods of each net are represented by different colors.

primitive cubic (α-Po) topology. A representation of a cuboid unit within this network is presented in Fig. 1b. Three crystallographically equivalent, interpenetrating networks are present in the crystal structure. A schematic representation of the interpenetrating network is presented in Fig. 1c.

The bpe ligand pairs serve as bipillars in the network of **1** and are arranged in a face-to-face fashion with a distance of 3.77 Å between C=C bonds of the neighbouring ligands. According to Schmidt's topochemical criteria, such a separation offers the prospect of a photochemical [2+2] cycloaddition reaction occurring between neighbouring molecules. Exposure of crystals of **1** to UV irradiation for 450min leads to the photodimerization of bpe ligands to give the stereospecific cycloaddition product, *rctt*-tetra(4-pyridyl)cyclobutane (*rctt*-tpcb, *rctt* indicates the orientations of the four groups on the cyclobutane ring are *cis*, *trans*, *trans*) (Supplementary Fig. S3) within the framework structure of $[Ni_3(oba)_2(rctt\text{-tpcb})(SO_4)(H_2O)_4]\cdot H_2O$ (**2**). Its PXRD patterns were similar to those of **1** though the intensities of some peaks were affected (Supplementary Fig. S2). For example, peaks at 6.80 and 6.94° were diminished in intensity while those of the peaks at 17.5 and 20.5° were enhanced. The results suggest that the main structural features of **1** are retained after UV exposure to form **2**. The ^{1}H NMR spectrum of the components of **2**, dissolved in solution as indicated in the experimental section, showed the disappearance of the signal due to the olefin protons at 7.58 ppm and the appearance of the signal due to cyclobutane protons at 4.66 ppm. Furthermore, shifts of the signals of the pyridyl protons from 8.60 to 8.32 ppm and from 7.6 ppm to 7.22 ppm confirmed 100% conversion of bpe into *rctt*-tpcb (Figure 2). The TGA of **2** showed that the lattice water molecule was lost at 180°C, whilst the coordinated water molecules were removed above 250°C (obsd. 8.15, calcd. 7.26%) (Supplementary Fig. S4). Following loss of water molecules, this compound appears to be stable up to 400°C; mass losses in the range 400 to 520°C are attributed to the ligand loss/decomposition leading to the final product NiO.

A single crystal X-ray structural analysis of **2** reveals similar cell dimensions to those found for **1** as well as the adoption of the same space group. General structural features are retained in the generation of **2** including the geometry of the trinuclear cluster however there are significant changes associated with the transformation of pairs of bpe ligands to *rctt*-tpcb ligands (Supplementary Fig. S5). The distance of the C=C bond in bpe is elongated from 1.312Å to 1.538Å following the formation of the C-C bond within the cyclobutane ring. The newly formed two C-C bonds (1.590Å) are comparable to those reported in the literature (1.587Å ~ 1.606Å)[55]. The two pyridyl rings from the neighbouring bpe ligands that were previously aligned parallel to each other now diverge from the cyclobutane ring. The Ni-*rctt*-tpcb-Ni distance is slightly shorter than the Ni-bpe-Ni distance in the precursor (Supplementary Table S2). The nature of the interpenetration is preserved following the formation of the cyclobutane rings (Supplementary Fig. S6). Overall, the transformation is accompanied by a small reduction in cell volume (by 0.6%). Thermogravimetric analysis shows that the water lattice molecules present in **1** are retained during the irradiation with UV light.

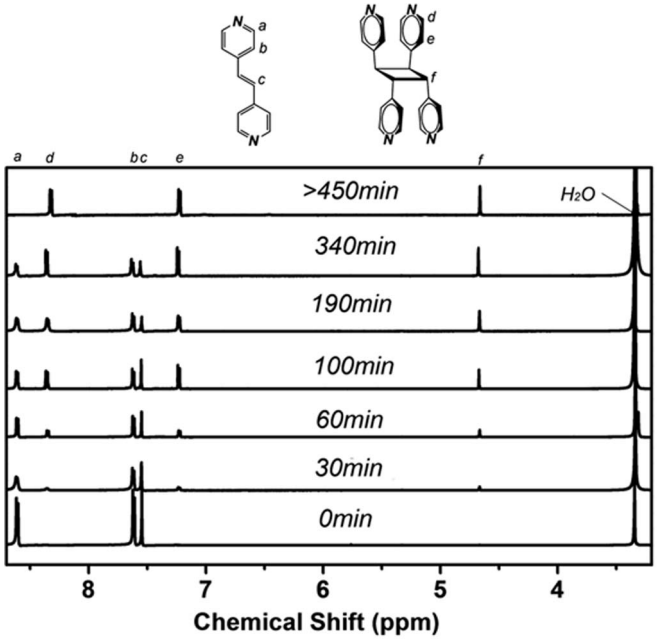

Figure 2 | ^{1}H NMR spectra of the samples of 1 irradiated by UV light within different irradiation time intervals.

There are limited examples of high-dimensional coordination polymers in which bpe or its derivatives are oriented in pairs. Gao *et al.* observed 60% photodimerization of the pillar-layered coordination polymer of composition $[Mn_2(HCO_2)_3(bpe)_2(H_2O)_2]ClO_4\cdot H_2O\cdot bpe$[56], however, in this case, photocycloaddition occurred between one type of bridging bpe and a lattice bpe that was held in place by hydrogen bonding. Subsequently, Vittal and co-workers reported a beautiful example of a photocycloaddition reaction occurring between parallel, coordinated bpe ligands within an interpenetrating 3D coordination polymer[49]. To our knowledge, the results described herein represent one of very few examples of a 3D→3D SCSC transformation of coordination polymers induced by UV light.

When a sample of **2** is heated to 180° to remove the lattice water molecules, it leads to the generation of compound **2a**. A single crystal X-ray structural analysis revealed that the framework structure of **2** is preserved upon loss of the lattice water. When **2a** is left in humid air for 3 days, water molecules return to the crystal structure. According to X-ray diffraction analysis this hydration-dehydration process is reversible. However, when **2a** is heated at 250°C for 2h, cracks in the crystal occur, which accompany a loss of crystallinity.

Kinetic analysis of photodimerization. In order to determine the kinetics of this reaction, we monitored the SCSC reaction and the corresponding structural transformation upon UV irradiation by *in situ* single-crystal X-ray analysis. When samples are exposed to unfiltered light from a high-pressure mercury lamp, producing UV radiation, significant structural changes are observed in **1** as indicated by PXRD patterns (Supplementary Fig. S2). Figure 3 depicts the transformation of the bpe to cyclobutane ring upon UV irradiation. These changes were monitored by collecting X-ray data sets after different periods of exposure to UV radiation. The structural refinement process using *SHELXTL* allowed refinement of the site occupancies of the atoms belonging to both the disappearing bpe ligands and the emerging tpcb ligands. This process allows the progress of the reaction in the crystal to be followed. There are many factors that may influence the photochemical kinetic study, such as the heat produced by the UV irradiation, the light flux of the UV lamp used, the light scattering, and the sizes of the single-crystal and the powder samples. Taking into these factors into consideration, we designed a UV light irradiation system (Supplementary Fig. S7). There is a cooling water system that can absorb the maximum heat from the UV irradiation. Each sample is placed into a glass plate that is also cooled by a cooling water system. The temperature at the sample can be kept at *ca.* 25°C. The distance between the crystal and the UV source was fixed to be 10 cm with the light flux of 37.55 mw/cm^2 or 20 cm with the light flux of 12.95 mw/cm^2. In addition, because the single-crystal and the powder samples absorb the UV light, it may cause the product gradient in the direction normal to the surface of the sample. The product gradient may be different for the single-crystal and the powder samples. Thus we tried to make the same thickness (*ca.* 0.2 mm) for both samples. Plots showing the

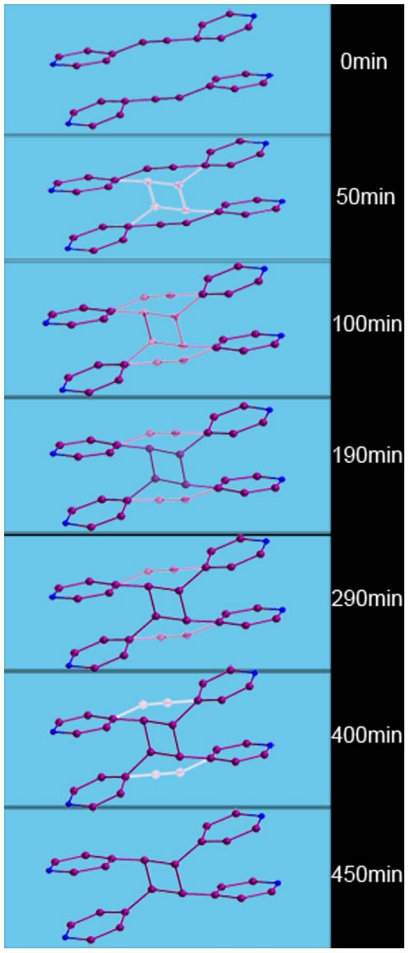

Figure 3 | Photocyclodimerization of the bpe ligands in single crystals of 1 over the course of the UV irradiation. The purple spheres and connections of the olefin and cyclobutane components represent higher occupancy while other paler colours correspond to lower occupancy.

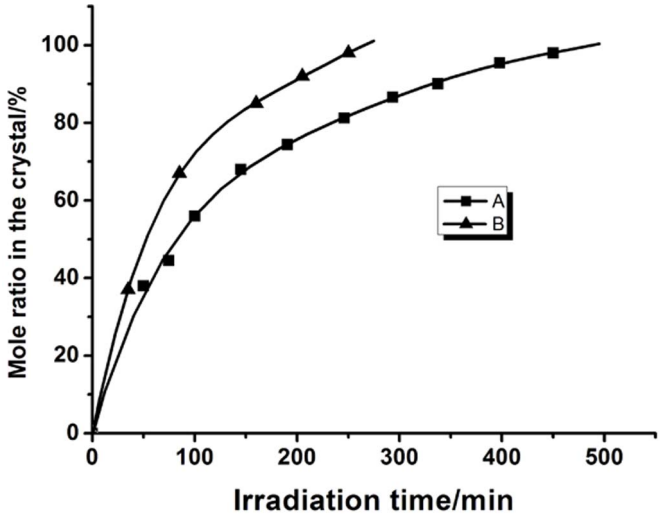

Figure 4 | Plots showing the percentage of bpe converted to *rctt*-tpcb in the single crystal sample **1** with irradiation time; A: Data corresponding to a lamp-to-sample separation of 20 cm with the light flux of 12.95 mw/cm^2; B: Data corresponding to a lamp-to-sample separation of 10 cm with the light flux of 37.55 mw/cm^2.

percentage conversion of bpe dimers to tpcb *versus* time are presented in Fig. 4.

Figure 4 indicates that exposure of a crystal to UV radiation for a period of 70 min (**1(70 min)**), leads to a 45% conversion of bpe ligands to *rctt*-tpcb ligands (see **1(70 min)** in Fig. 3 and Supplementary Table S3). After 240 min, the reaction was found to be 80% complete (see **1(240 min)** in Fig. 4) and after 450 min (see **1(450 min)** in Fig. 3), the reaction is essentially complete. This process could also be followed by monitoring the change in separation between Ni(II) centres that are initially bridged by bpe ligands (Supplementary Table S2 and S4, Fig. S8 and S9). The course of the photocycloaddition of **1** under UV light was also monitored by measuring the ^{1}H NMR spectra of the crystal components dissolved in DMSO-d_6 (Supplementary Fig. S10 to S20), which were extracted using the method (see Supplementary Information). Inspection of Fig. 2 reveals that over a period in excess of 450 min the sharp olefinic signal at 7.58 ppm disappears to be replaced by the characteristic cyclobutane protons at 4.66 ppm (Fig. 2). Analysis of the data indicated the first order kinetics with rate constants of 12.55×10^{-3} min^{-1} and 7.14×10^{-3} min^{-1}, being obtained for lamp-to-sample separations of 10 and 20 cm with the light flux of 37.55 and 12.95 mw/cm^2, respectively (Fig. 5a and 5b). The results are identical to those reported previously[27–28].

Discussion

In this work reported here, we have prepared a 3D coordination polymer **1** from the solvothermal reactions of $NiSO_4$ with oba and bpe. Compound **1** has been shown to undergo a SCSC structural transformation in which upon UV irradiation, bpe ligands are converted into *rctt*-tpcb ligands within a 3D network, yielding compound **2**. We have used *in situ* single-crystal X-ray diffraction snapshots to probe the reaction kinetics, which showed the first-order reaction behavior. The results are consistent with those obtained from ^{1}H NMR spectra. We have also been able to confirm that the rate of the photoreaction is dependent upon the separation between the sample and the light source. To our knowledge, this is the first time that the rate order of a [2+2] photocycloaddition reaction in the solid state has been determined by *in-situ* X-ray diffraction snapshotting, with first order behavior being observed. It is anticipated that this methodology may be applied to examine the kinetics and mechanisms of photoreactions within single crystals of other compounds in which the rate of transformation is similar to that reported here.

Methods

General. Ligands (H_2oba and bpe) and other metal salts were obtained commercially and used without further purification. Elemental analyses (C, H, and N) were performed using a PE 2400 II elemental analyzer. The FT-IR spectra were recorded with a Nicolet Mana-IR 550 spectrometer in dry KBr disks in the 400–4000 cm^{-1} range. The thermogravimetric analyses (TGA) were performed using a Mettler TGA/SDTA851 thermal analyzer under an N_2 atmosphere with a heating rate of 10°C/min in the temperature region of 20-800°C. Powder X-ray diffraction (XRD) patterns were collected on a Bruker D8 advance diffractometer using graphite monochromatized Cu Kα radiation (λ = 1.5406 Å). The UV-irradiation experiments were conducted with a high-pressure mercury lamp and a radiation with λ = 365 nm.

Preparation of $[Ni_3(oba)_2(bpe)_2(SO_4)(H_2O)_4]\cdot H_2O$ (1). To a thick Pyrex tube was loaded $NiSO_4\cdot 7H_2O$ (280 mg, 1 mmol),H_2oba (258 mg, 1 mmol), bpe (182 mg, 1 mmol) and 2 mL of DMF and H_2O (v/v = 4:6). The tube was sealed and then heated at 145°C for 120 h. After it was cooled to room temperature at a rate of 5°C/h, green crystals of **1** were formed, which were collected by filtration, washed with EtOH and Et_2O, and dried in air. Yield: 718 mg (58% based on $NiSO_4\cdot 7H_2O$). IR (KBr disk,): 3447, 1614, 1600, 1553, 1408, 1336, 1236, 1142, 980, 825, 785 cm^{-1} (Supplementary Fig. S21); analysis (calcd., found for $C_{52}H_{46}N_4Ni_3O_{19}S$): C (50.40, 50.29), H (3.74, 3.64), N (4.52, 4.58).

Preparation of $[Ni_3(oba)_2(rctt\text{-}tpcb)(SO_4)(H_2O)_4]\cdot H_2O$ (2). Single crystals of **1** (500 mg) in between glass slides were irradiated with a Hg lamp for *ca.* 450 min to form **2** in 100% yield based on **1**. IR (KBr disk): 3446, 1612, 1603, 1551, 1402, 1339, 1235, 1142, 985, 822, 783 cm^{-1} (Supplementary Fig. S22); analysis (calcd., found for $C_{52}H_{46}N_4Ni_3O_{19}S$): C (50.40, 50.33), H (3.74, 3.66), N (4.52, 4.54).

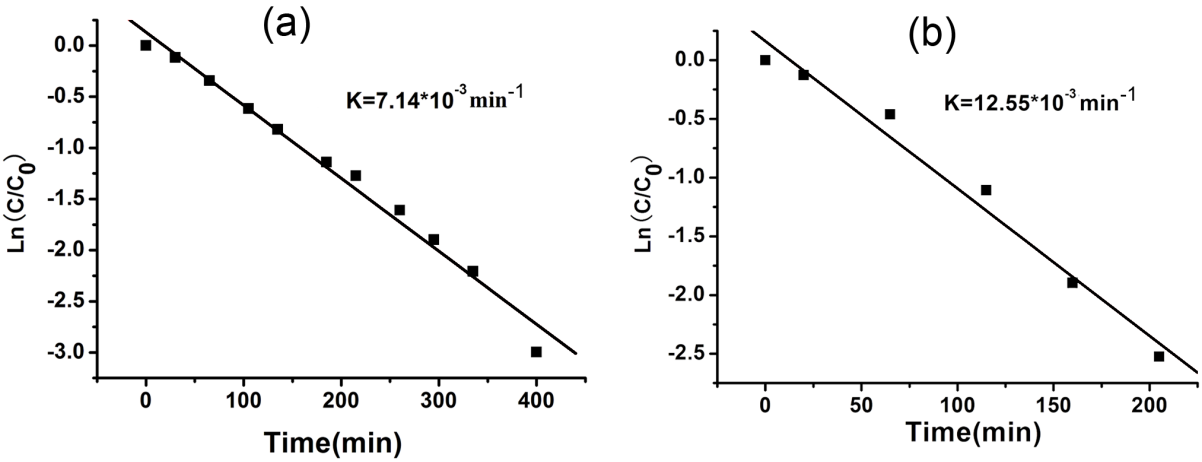

Figure 5 | Plots of ln(C/C$_0$) versus time indicating first order behaviour; C/C$_0$ represents the fraction of bpe converted to *rctt*-tpcb: (a) Data corresponding to a lamp-sample separation of 20 cm; (b) Data corresponding to a lamp-sample separation of 10 cm.

Preparation of [Ni$_3$(oba)$_2$(*rctt*-tpcb)(SO$_4$)(H$_2$O)$_4$] (2a). Single crystals of **2** were heated at 180°C in the oil bath for 2 h to give compound **2a**. IR (KBr disk): 3446, 1614, 1600, 1553, 1408, 1331, 1232, 1148, 981, 827, 784 cm^{-1} (Supplementary Fig. S23); analysis (calcd., found for $C_{52}H_{44}N_4Ni_3O_{18}S$): C (51.15, 51.19), H (3.63, 3.64), N (4.59, 4.56).

UV irradiation. Single crystals: One single crystal of **1** was sealed in a glass tube and irradiated with a high-pressure mercury lamp at ambient temperature. The distance between each sample and the UV light source was fixed to be 20 cm with the light flux of 12.95 mw/cm^2. The single crystal X-ray diffraction was used to monitor the ratio of bpe/*rctt*-tpcb in each sample within the different irradiation time intervals (50 min, 70 min, 100 min, 145 min, 190 min, 240 min, 290 min, 340 min, 400 min and 450 min). The other single crystal of **1** was sealed in a glass tube and irradiated with high-pressure mercury lamp at ambient temperature for 30 min, 80 min, 160 min, 200 min and 250 min, respectively. However, the distance between the single-crystal sample and the UV light source was fixed to be 10 cm with the light flux of 37.55 mw/cm^2. The aforementioned same procedure was repeated for each sample.

Powder crystals: The crystals were firmly ground into small particles and then spread evenly on a glass plate. Each sample was turned over frequently to receive the maximum uniform irradiation. The distance between each sample and the UV light source was fixed to be 20 cm with the light flux of 12.95 mw/cm^2. The samples were divided into 10 parts, each of which was exposed to the UV light for a different time interval (50 min, 70 min, 100 min, 145 min, 190 min, 240 min, 290 min, 340 min, 400 min and 450 min). The photoproduct in each irradiated part was extracted using the method (see Supplementary Information) for the ^{1}H NMR identification.

Isolation of bpe and other photoproducts formed at different irradiation time intervals. A mixture containing $Na_2(H_2edta)\cdot 2H_2O$ (1.8 g, 5 mmol), **1** or each other sample obtained from UV irradiation over **1** for 50 min, 70 min, 100 min, 145 min, 190 min, 240 min, 290 min, 340 min, 400 min or 450 min (1.24 g, 1 mmol), NaOH (0.2 g, 5 mmol), H_2O (40 mL) and CH_2Cl_2 (40 mL) was placed in a 150 mL flask and stirred for one day. The organic phase was separated from the reaction mixture and the aqueous layers were also extracted using CH_2Cl_2 (4 × 30 mL). The combined organic extract was concentrated to dryness *in vacuo*. The resulting sample was then washed thoroughly with NaOH solution and H_2O, and dried with anhydrous Na_2SO_4 to give bpe or other intermediate photoproduct as a yellow powder which was used for the ^{1}H NMR measurement.

1. Georgiev, I. G. & MacGillivray, L. R. Metal-mediated reactivity in the organic solid state: from self-assembled complexes to metal-organic frameworks. *Chem. Soc. Rev.* **36**, 1239–1248 (2007).
2. Nandi, G. & Sarkar, S. Solid-state synthesis of molybdenum and tungsten porphyrins and aerial oxidation of coordinated benzenethiolate to benzenesulfonate. *Inorg. Chem.* **51**, 6412–6420 (2012).
3. MacGillivray, L. R. *et al.* Supramolecular control of reactivity in the solid state: from templates to ladderanes to metal-organic frameworks. *Acc. Chem. Res.* **41**, 280–291 (2008).
4. Vittal, J. J. Supramolecular structural transformations involving coordination polymers in the solid state. *Coord. Chem. Rev.* **251**, 1781–1795 (2007).
5. Tanaka, K. & Toda, F. Solvent-free organic synthesis. *Chem. Rev.* **100**, 1025–1074 (2000).
6. Yamada, S., Uematsu, N. & Yamashita, K. Role of cation-π interactions in the photodimerization of *trans*-4-styrylpyridines. *J. Am. Chem. Soc.* **129**, 12100–12101 (2007).
7. Papaefstathiou, G. S., Zhong, Z. M., Geng, L. & MacGillivray, L. R. Coordination-driven self-assembly directs a single-crystal-to-single-crystal transformation that exhibits photocontrolled fluorescence. *J. Am. Chem. Soc.* **126**, 9158–9159 (2004).
8. Vitórica-Yrezábal, *et al* Chemical transformations of a crystalline coordination polymer: a multi-stage solid-vapour reaction manifold. *Chem. Sci.* **4**, 696–708 (2013).
9. Bardelang, D. *et al.* Single-crystal to single-crystal phase transition of cucurbit[5]uril hydrochloride hydrates: large water-filled channels transforming to layers of unusual stability. *Chem. Commun.* 4927–4929 (2008).
10. Wen, L., Cheng, P. & Lin, W. B. Solvent-induced single-crystal to single-crystal transformation of a 2D coordination network to a 3D metal–organic framework greatly enhances porosity and hydrogen uptake. *Chem. Commun.* **48**, 2846–2848 (2012).
11. Yan, B., Shi, R., Zhang, B. & Kshirsagar, T. A kinetic study of product cleavage reactions from the solid phase by a biocompatible and removable cleaving reagent, HCl. *J. Comb. Chem.* **9**, 684–689 (2007).
12. Lan, P., Porco, J. A., South, M. S. & Parlow, J. J. Quality control in combinatorial chemistry: determination of the quantity, purity, and quantitative purity of compounds in combinatorial libraries. *J. Comb. Chem.* **5**, 660–669 (2003).
13. Yan, B. Monitoring the progress and the yield of solid-phase organic reactions directly on resin supports. *Acc. Chem. Res.* **31**, 621–630 (1998).
14. Kitagawa, S. & Uemera, K. Dynamic porous properties of coordination polymers inspired by hydrogen bonds. *Chem. Soc. Rev.* **34**, 109–119 (2005).
15. Han, Y. F., Jin, G. X. & Hahn, F. E. Postsynthetic modification of dicarbene-derived metallacycles via photochemical [2+2] cycloaddition. *J. Am. Chem. Soc.* **135**, 9263–9266 (2013).
16. Seo, J., Matsuda, R., Sakamoto, H., Bonneau, C. & Kitagawa, S. A pillared-layer coordination polymer with a rotatable pillar acting as a molecular gate for guest molecules. *J. Am. Chem. Soc.* **131**, 12792–12800 (2009).
17. Chippindale, A. M. & Hibble, S. J. Helices, Chirality and interpenetration: the versatility and remarkable interconversion of silver-copper cyanide frameworks. *J. Am. Chem. Soc.* **131**, 12736–12744 (2009).
18. Park, I. H. *et al.* Metal-organic organopolymeric hybrid framework by reversible [2+2] cycloaddition reaction. *Angew. Chem. Int. Ed.* **53**, 414–419 (2014).
19. Ranford, J. D., Vittal, J. J. & Wu, D. Q. Topochemical conversion of a hydrogen-bonded three-dimensional network into a covalently bonded framework. *Angew. Chem. Int. Ed.* **37**, 1114–1116 (1998).
20. Chu, Q., Swenson, D. C. & MacGillivray, L. R. A single-crystal-to-single-crystal transformation mediated by argentophilic forces converts a finite metal complex into an infinite coordination network. *Angew. Chem. Int. Ed.* **44**, 3569–3572 (2005).
21. Cheng, X. N., Zhang, W. X. & Chen, X. M. Single crystal-to-single crystal transformation from ferromagnetic discrete molecules to a spin-canting antiferromagnetic layer. *J. Am. Chem. Soc.* **129**, 15738–15739 (2007).
22. Ghosh, S. K., Bureekaew, S. & Kitagawa, S. A dynamic, isocyanurate-functionalized porous coordination polymer. *Angew. Chem. Int. Ed.* **47**, 3403–3406 (2008).
23. Kawamichi, T., Haneda, T., Kawano, M. & Fujita, M. X-ray observation of a transient hemiaminal trapped in a porous network. *Nature* **461**, 633–635 (2009).
24. MacGillivray, L. R. On substituents, steering, and stacking to control properties of the organic solid state. *CrystEngComm* **6**, 77–78 (2004).
25. Yang, S. Y. *et al.* Crystallographic snapshots of the interplay between reactive guest and host molecules in a porous coordination polymer: stereochemical coupling and feedback mechanism of three photoactive centers triggered by UV-induced isomerization, dimerization, and polymerization reactions. *J. Am. Chem. Soc.* **136**, 558–561 (2014).

26. Nagarathinam, M., Peedikakkal, A. M. P. & Vittal, J. J. Stacking of double bonds for photochemical [2+2] cycloaddition reactions in the solid state. *Chem. Commun.* 5277–5288 (2008).
27. Medishetty, R. *et al.* Single crystals popping under UV light: A photosalient effect triggered by a [2+2] cycloaddition reaction. *Angew. Chem. Int. Ed.* **53**, 5907–5911 (2014).
28. Bertmer, M., Nieuwendaal, R. C., Barnes, A. B. & Hayes, S. E. Solid-State photodimerization kinetics of α-trans-cinnamic acid to α-truxillic acid studied via solid-state NMR. *J. Phys. Chem. B.* **110**, 6270–6273 (2006).
29. Enkelmann, V. & Wegner, G. Single-crystal-to-single-crystal photodimerization of cinnamic acid. *J. Am. Chem. Soc.* **115**, 10390–10391 (1993).
30. Sreevidya, T. V., Cao, D. K., Lavy, T., Botoshansky, M. & Kaftory, M. Unexpected molecular flip in solid-state photodimerization. *Cryst. Growth Des.* **13**, 936–941 (2013).
31. Fonseca, I., Hayes, S. E., Blümich, B. & Bertmer, M. Temperature stability and photodimerization kinetics of *β*-cinnamic acid and comparison to its α-polymorph as studied by solid-state NMR spectroscopy techniques and DFT calculations. *Phys. Chem. Chem. Phys.* **10**, 5898–5907 (2008).
32. Garai, D., Santra, R. & Biradha, K. Tunable plastic films of a crystalline polymer by single-crystal-to-single-crystal photopolymerization of a diene: self-templating and shock-absorbing two-dimensional hydrogen-bonding layers. *Angew. Chem. Int. Ed.* **52**, 5548–5551 (2013).
33. Peedikakkal, A. M. P., Koh, L. L. & Vittal, J. J. Photodimerization of a 1D hydrogen-bonded zwitterionic lead(II) complex and its isomerization in solution. *Chem. Commun.* 441–443 (2008).
34. Vela, M. J., Buchholz, V., Enkelmann, V., Snider, B. B. & Foxman, B. M. Solid-state polymerization of bis(but-3-enoato)zinc: the generation of a stereoregular oligomer. *Chem. Commun.* 2225–2226 (2000).
35. Gao, X., Friščić, T. & MacGillivray, L. R. Supramolecular construction of molecular ladders in the solid state. *Angew. Chem. Int. Ed.* **43**, 232–236 (2004).
36. Dushyant, B., Papaefstathiou, G. & MacGillivray, L. R. Site-directed regiocontrolled synthesis of a 'head-to-head' photodimer via a single-crystal-to-single-crystal transformation involving a linear template. *Chem. Commun.* 1964–1965 (2002).
37. Qu, Y. C., Zhi, D. S., Liu, W. T., Ni, Z. P. & Tong, M. L. Single-crystal-to-single-crystal transformation from 1 D staggered-sculls chains to 3 D NbO-type metal-organic framework through [2+2] photodimerization. *Chem. Eur. J.* **18**, 7357–7361 (2012).
38. Li, J. *et al.* Metal-organic frameworks displaying single crystal-to-single crystal transformation through postsynthetic uptake of metal clusters. *Chem. Sci.* **4**, 3232–3238 (2013).
39. Xu, R., Gramlich, V. & Frauenrath, H. Alternating diacetylene copolymer utilizing perfluorophenyl-phenyl interactions. *J. Am. Chem. Soc.* **128**, 5541–5547 (2006).
40. Lee, S. B., Koepsel, R., Stolz, D. B., Warriner, H. E. & Russell, A. J. Self-assembly of biocidal nanotubes from a single-chain diacetylene amine salt. *J. Am. Chem. Soc.* **126**, 13400–13405 (2004).
41. Peng, H. *et al.* Polydiacetylene/silica nanocomposites with tunable mesostructure and thermochromatism from diacetylenic assembling molecules. *J. Am. Chem. Soc.* **127**, 12782–12783 (2005).
42. Coates, G. W. *et. al.* Phenyl-perfluorophenyl stacking interactions: topochemical [2+2] photodimerization and photopolymerization of olefinic compounds. *J. Am. Chem. Soc.* **120**, 3641–3649 (1998).
43. Li, Z., Fowler, F. W. & Lauher, J. W. Electrochemistry and electrogenerated chemiluminescence of 3,6-di(spirobifluorene)-N-phenylcarbazole. *J. Am. Chem. Soc.* **130**, 634–639 (2008).
44. Lauher, J. W., Fowler, F. W. & Goroff, N. S. Single-crystal-to-single-crystal topochemical polymerizations by design. *Acc. Chem. Res.* **41**, 1215–1229 (2008).
45. Xiao, J., Yang, M., Lauher, J. W. & Fowler, F. W. A supramolecular solution to a long-standing problem: the 1,6-polymerization of a triacetylene. *Angew. Chem. Int. Ed.* **39**, 2132–2135 (2000).
46. Zhao, D., Timmons, D. J., Yuan, D. Q. & Zhou, H. C. Tuning the topology and functionality of metal-organic frameworks by ligand design. *Acc. Chem. Res.* **44**, 123–133 (2011).
47. Nomura, S. *et al.* Crystal structures and topochemical polymerizations of 7,7,8,8-tetrakis(alkoxycarbonyl)- quinodimethanes. *J. Am. Chem. Soc.* **126**, 2035–2041 (2004).
48. Hagrman, P. J., Hagrman, D. & Zubieta, J. Organic-inorganic hybrid materials: from "simple" coordination polymers to organodiamine-templated molybdenum oxides. *Angew. Chem. Int. Ed.* **38**, 2638–2684 (1999).
49. Mir, M. H., Koh, L. L., Tan, G. K. & Vittal, J. J. Single-crystal to single-crystal photochemical structural transformations of interpenetrated 3D coordination polymers by [2+2] cycloaddition reactions. *Angew. Chem. Int. Ed.* **122**, 400–403 (2010).
50. Kole, G. K. & Vittal, J. J. Solid-state reactivity and structural transformations involving coordination polymers. *Chem. Soc. Rev.* **42**, 1755–1775 (2013).
51. Benedict, J. B. & Coppens, P. Kinetics of the single-crystal to single-crystal two-photon photodimerization of α-trans-cinnamic acid α-truxillic acid. *J. Phys. Chem. A.* **113**, 3116–3120 (2009).
52. Cao, D. K. *et al.* Kinetics of solid state photodimerization of 1,4-dimethyl-2-pyridinone in its molecular compound. *J. Phys. Chem. A.* **114**, 7377–7381 (2010).
53. Bertmer, M., Nieuwendaal, R. C., Barnes, A. B. & Hayes, S. E. Solid-state photodimerization kinetics of α-trans-cinnamic acid to α-truxillic acid studied via solid-state NMR. *J. Phys. Chem. B.* **110**, 6270–6273 (2006).
54. Fonseca, I., Hayes, S. E. & Bertmer, M. Size effects of aromatic substitution in the *ortho* position on the photodimerization kinetics of α-transcinnamic acid derivatives. A solid-state NMR study. *Phys. Chem. Chem. Phys.* **11**, 10211–10218 (2009).
55. Toh, N. L., Nagarathinam, M. & Vittal, J. J. Topochemical photodimerization in the coordination polymer $[\{(CF_3CO_2)(\mu\text{-}O_2CCH_3)Zn\}_2(\mu\text{-bpe})_2]_n$ through single-crystal to single-crystal transformation. *Angew. Chem., Int. Ed.* **44**, 2237–2241 (2005).
56. Wang, X. Y., Wang, Z. M. & Gao, S. A pillared layer MOF with anion-tunable magnetic properties and photochemical [2+2] cycloaddition. *Chem. Commun.* 1127–1129 (2007).

Acknowledgments

J.P.L. acknowledges the financial supports from the National Nature Science Foundation of China (21171124 and 21371126), State Key Laboratory of Organometallic Chemistry, Shanghai Institute of Organic Chemistry, Chinese Academy of Sciences (201201006), the Qin-Lan Project and the "333" Project of Jiangsu Province, the Priority Academic Program Development of Jiangsu Higher Education Institutions, and the "SooChow Scholar" Program of Soochow University. Innovative Research Program for Postgraduates in Universities of Jiangsu Province (KYZZ-0335) and Guangxi Natural science foundation (2014GXNSFBA118044).

Author contributions

J.P.L. supervised the project. F.L.H. conceived and carried out experiments, determined structures, analysed data and wrote the paper. S.L.W. assisted in the solvothermal synthesis and structural characterization of the title compounds. J.P.L. designed the study, analysed data and wrote the paper. B.F.A. analysed data and wrote the paper.

Additional information

Accession codes: The X-ray crystallographic data and refinement parameters for all the structures reported in this article (see Supplementary Table S1) have been deposited at the Cambridge Crystallographic Data Centre (CCDC) under deposition numbers CCDC 1013370 [**1(0 min)**], 1013371 [**1(50 min)**], 1013372 [**1(70 min)**], 1013373 [**1(100 min)**], 1013374 [**1(145 min)**], 1013375 [**1(190 min)**], 1013376 [**1(240 min)**], 1013377 **1(290 min)**, 1013378 [**1(340 min)**], 1013379 [**1(400 min)**], 1013380 [**1(450 min)**], CCDC 1013381 [**1'(0 min)**], 1013382 [**1'(30 min)**], 1013383 [**1'(80 min)**], 1013384 [**1'(160 min)**], 1013385 [**1'(200 min)**], 1013386 [**1'(250m in)**] and 983179 [**2a**]. These data can be obtained free of charge from the Cambridge Crystallographic Data Centre via http://www.ccdc.cam.ac.uk/data_request/cif.

Supplementary information accompanies this paper at http://www.nature.com/scientificreports

Competing financial interests: The authors declare no competing financial interests.

How to cite this article: Hu, F.-L., Wang, S.-L., Lang, J.-P. & Abrahams, B.F. *In-situ* X-ray diffraction snapshotting: Determination of the kinetics of a photodimerization within a single crystal. *Sci. Rep.* **4**, 6815; DOI:10.1038/srep06815 (2014).